CHAOS VOLUME 14, NUMBER 1 MARCH 2004

# Stability and the maintenance of balance following a perturbation from quiet stance

J. R. Stirling[a] and M. S. Zakynthinaki[b]
*Centre de Recerca Matemàtica, Apartat 50, E-08193 Bellaterra, Barcelona, Spain*

(Received 9 May 2003; accepted 2 October 2003; published online 14 November 2003)

We investigate stability and the maintenance of balance with the use of tools from dynamical systems. In particular we investigate the application of such tools to the study of the ground reaction forces resulting from an athlete being perturbed from quiet stance. We develop a nonlinear model consisting of a set of coupled vector fields for the derivative with respect to time of the angles between the resultant ground reaction forces and the vertical in the anteroposterior and mediolateral directions. This model contains a basin of attraction bound by a closed curve which we call the critical curve. It is only inside this curve that perturbations can be corrected, with the orbit spiraling onto an attractor corresponding to quiet stance. We show how the critical curve and also the strength of the attractor found in the basin of attraction can be fit to model the experimental data (time series) for an individual athlete. We also discuss how our model can be used to identify nonsymmetric behavior caused by muscle imbalances and differences in the ranges of motion on either side of the body. © *2004 American Institute of Physics.* [DOI: 10.1063/1.1628451]

**We use tools from dynamical systems (see, for example, Kantz and Schreiber[1] and Guckenheimer and Holmes[2]) to investigate and model the stability or maintenance of balance of an athlete perturbed from quiet stance while standing on a force platform. We show how the model can be fit to individual athletes and be used to identify nonsymmetric behavior resulting from muscle imbalances and other causes. Stability and reproducibility of a pattern of movement following a perturbation is critical to success in many sports (Marin *et al.*,[3] Vuillerme *et al.*,[4] Riccio and Stoffregen,[5] and Mester[6]) and other areas of life. A model such as the one we present here would be of much use for detecting improvements in balance brought on by training.**

## I. INTRODUCTION

Balance in quiet upright stance does not imply motionless stability,[7–19] in fact a mediolateral and anteroposterior body sway occurs. The two types of body sways are regulated by two independent subsystems with different but reciprocal dynamics. These two independent subsystems control either the anteroposterior sway (AP) or the mediolateral sway (ML) (Winter *et al.*[20] and Balasubramaniam *et al.*[21]). Nashner and co-workers (see Nashner,[22] Nashner and McCollum,[23] Horak and Nashner,[24] and McCollum and Leen[25]) have emphasized that almost 95% of the anterior–posterior sway happens around the ankle and the hip axis in situations such as we present here. They ran experiments reporting that the postural system reduces the high number of degrees of freedom by compressing them into two muscular synergies described at the neuromuscular level. The two synergies are termed the ankle and hip strategies. More recently, Bardy and co-workers (see Bardy *et al.*[26,27] and Oullier *et al.*[18]) have shown that the relative motion of the ankles and the hips in postural oscillations exhibit typical hallmarks of dynamical systems, this includes relaxation time after perturbation (see Bardy *et al.*[27]). The ankle controls the shifts of the center of mass via rotating about the feet. In terms of postural sway, the knee does not play as important a role as the hip. Lateral and forward–backward movements of the hip are used to control the center of mass (Lekhel *et al.*[28]), whilst the role played by the knee is mainly to resist gravity (Massion[29] and Bouisset[30]).

The coordination of the human body can be thought of as a result of a highly complicated interaction of many variables (muscular and neurological) and the constraints applied to them. Local constraints such as central command signals or forces and also other environmental, intrinsic, and intentional constraints have been shown to play an important role in shaping patterns of whole-body coordination, such as postural pattern formation (see Newell[31] and Kelso[32]). Regarding modelling the coordination of the human body, Bernstein[33] and Kelso[32] showed the problems associated with mixing levels of descriptions, for example, extrapolating the kinematics of the coordination after only recording the kinetics. In order to discuss kinetics, therefore, one has to measure kinetics, which is what we do in the following sections of this paper by modelling and measuring only the time series of the ground reaction force. For an extended review of this point, applied to postural coordination, see Bardy *et al.*[27]

When one looks at the phase space for the dynamical system governing the angles between resultant ground reaction force and the vertical in the mediolateral and the anteroposterior directions, one can see that there exists a region where the subject is able to maintain balance without falling. We considered this region to be a basin of attraction. Static stability regions with respect to ankle and hip joints were

[a]Electronic mail: j.r.stirling@mailcity.com
[b]Electronic mail: marzak@mailcity.com

 

also proposed in Bardy *et al.*,[26] while McCollum and Leen[25] used a concept based on the mechanical limit of upright stance with respect to the angles of the ankle and the hip which they called the stability cone. The orientations and configurations, for which the organism is optimally maintained, will correspond to an attractor found within the basin of attraction. We simplify the nature of this attractor to be a complex sink. This is because the amplitudes of perturbations and movements of the body we consider are much larger than those due to body sway during quiet stance. When seen on this larger scale the low frequency motion back onto the body position occupied during quiet stance has the spiraling features of the motion onto a complex sink fixed point. The limiting orientations and configurations that will separate ultimately different body positions (i.e., upright stance versus horizontally lying on the floor) will define a closed curve called the critical curve, which will in turn define the bounds of the basin of attraction.

The reversal of postural perturbations is dependent on the ability to generate thrust at the support surface. This requires a support surface of adequate extent and rigidity as well as sufficient muscular force. If the postural perturbation produces a movement too far from the vertical the subject will abandon the specified foot position resulting in actions such as falling or taking a step to prevent falling (see Sims and Brauer[34] for experiments on stepping). The postural restoring response is a function of body morphology, muscular strength, and neurological condition. The size and shape of the basin of attraction and the strength of the attractor contained within, will therefore depend on the individual athlete and also their condition. Other factors such as constraints due to the task and to the environment (Newell[31]) will also have an effect.

In the following sections we present the data obtained from the force platform with an explanation of the relevant features of the time series. Using this we produce a model of the processes of maintaining balance. This is then analyzed with regards to the linear stability of the structures of interest in the phase space. We then provide conclusions including a series of practical implications for training and testing of stability in athletes (see Stirling and Zakythinaki[35] for more details especially regarding the application of the model to injury prevention). Sports in general provide examples of supra-postural tasks, i.e., tasks in which the achievement of stable posture is necessary but not the main goal, see Stoffregen *et al.*[36]

## II. EXPERIMENTAL PROCEDURE AND THE FORCE PLATFORM DATA

The experiment consisted of an athlete being perturbed from quiet stance while standing on a force platform (AMTI, digital recording frequency: 500 Hz). The perturbation was a result of the athlete being pushed (i.e., an impulse) in both a variety of directions and with a variety of forces. The athlete stood upright with feet aligned to the anteroposterior axis with hands on hips. Neither the feet nor the hands were allowed to change position for the restoration of balance to have been considered successful. Figure 1 shows a computer simulation of the posture of the athlete, during quiet stance and also when pushed in all four directions.[37]

The time series of the resultant ground reaction force exerted on the force platform was recorded as the athlete tried to regain balance following the perturbation. For the purposes of the present study the time series of the three forces $F_X, F_Y, F_Z$ are converted into time series of the two angles $\theta_X$ and $\theta_Y$, with $\theta_X$ being the angle of the resultant force $F$ from the vertical in $x$ anteroposterior direction, and $\theta_Y$ being the angle of the resultant force $F$ from the vertical in the $y$ mediolateral direction, see Fig. 2.

We present a plot of the time series of the angles $\theta_X$ and $\theta_Y$ (see Fig. 3) and also of the two angles plotted against each other (Fig. 4). One of the main features of these graphs is the presence of oscillations; the more unstable the body the larger the oscillation. It should be noted, however, that large oscillations can be considered to be stable under certain constraints (see Bardy *et al.*[27]). We make the claim that the large scale oscillations seen in Figs. 3 and 4 are due to the motion of the center of gravity of the body as it is perturbed to an unstable state (i.e., it is unbalanced or out of equilibrium) and then returns to quiet stance or in other words regains balance. We also make the claim that these oscillations die out as the body regains balance and is back onto the attractor. The length of time taken for this is a measure of the strength of the attractor.

## III. MODEL

We simplify the dynamics and do not take into account any small scale high frequency natural oscillations in the body (see Yoneda and Tokumasu[19]), hence our model is only of the large scale low frequency dynamics. We assume that the condition $\theta_X=\theta_Y=0$ corresponds to the vertical state and also that the condition $\theta_X^2+\theta_Y^2=\pi^2/4$ corresponds to the horizontal state. Failure (falling on the floor) is a result of the center of gravity being displaced too far from the vertical. Observation of the data reveals the presence of a loop of critical angles $\theta_X^c$ and $\theta_Y^c$, such that

(1) for values of $0\leqslant\theta_X\leqslant\theta_X^c$ and $0\leqslant\theta_Y\leqslant\theta_Y^c$ the athlete is able to regain stability;
(2) for values of $\theta_X^c<\theta_X\leqslant\pi/2$ and $\theta_Y^c<\theta_Y\leqslant\pi/2$ the athlete loses stability and ends up lying on the floor.

For the modelling of the restabilization process, a set of coupled vector fields is used to model the variables $\theta_X$ and $\theta_Y$. Our model (see also Fig. 5 which shows the proposed phase space) has

(a) an attracting fixed point at $\theta_X=\theta_Y=0$;
(b) a repelling set of fixed points corresponding to the critical state at $\theta_X^c$, $\theta_Y^c$; and
(c) an attracting set of fixed points at $\theta_X^2+\theta_Y^2=\pi^2/4$.

Taking into account the above remarks, the equations which describe the model can be expressed in the form

$$\dot{\theta}_X=-f_{ax}(\theta_X,\theta_Y)f_c(\theta_X,\theta_Y)f_f(\theta_X,\theta_Y), \quad (1)$$

$$\dot{\theta}_Y=-f_{ay}(\theta_X,\theta_Y)f_c(\theta_X,\theta_Y)f_f(\theta_X,\theta_Y), \quad (2)$$

where $\theta_X^2+\theta_Y^2\leqslant\pi^2/4$,

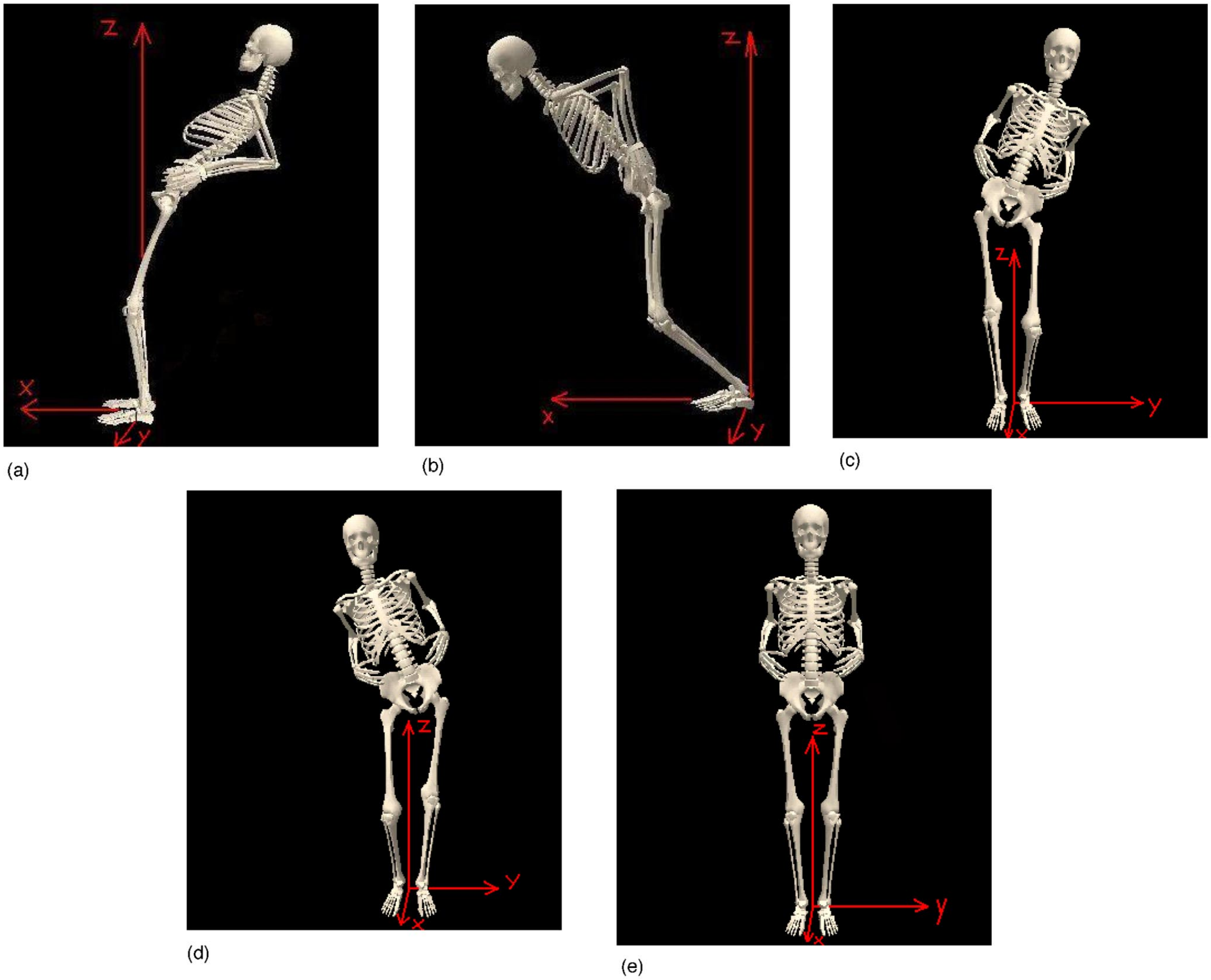


FIG. 1. (Color online) The simulated skeleton, adapted from a dynamical animation tool (Ref. 37), standing upright and leaning at a maximum angle in all $x$, $-x$, $y$, and $-y$ directions, after application of an external force in the corresponding directions.

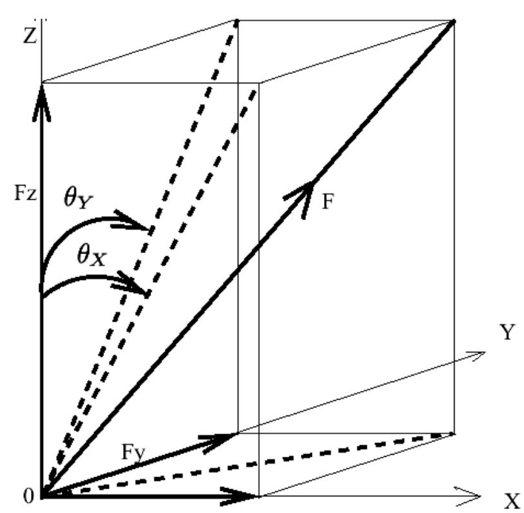


FIG. 2. The two angles $\theta_X$ and $\theta_Y$ between the resultant force $F$ and its three components $F_x, F_y, F_z$.

$$f_{ax}(\theta_X,\theta_Y) = -(\alpha\theta_X + \eta\theta_Y), \tag{3}$$

$$f_{ay}(\theta_X,\theta_Y) = -(\gamma\theta_X + \kappa\theta_Y), \tag{4}$$

$$f_f(\theta_X,\theta_Y) = \frac{\pi^2}{4} - \theta_X^2 - \theta_Y^2, \tag{5}$$

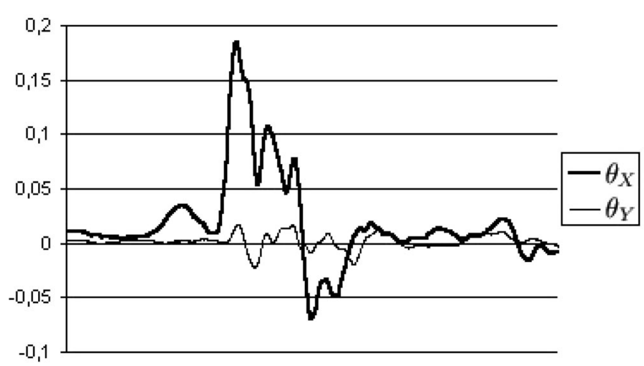


FIG. 3. Time series of the angles $\theta_X$ and $\theta_Y$ corresponding to the subject being pushed forwards. The horizontal axis represents time.

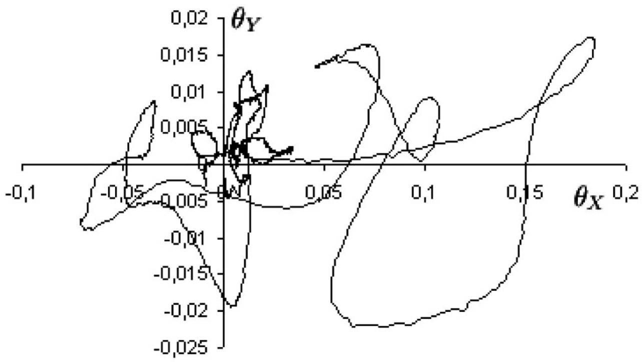


FIG. 4. The two angles $\theta_X$ and $\theta_Y$ plotted against each other. The spiraling is the result of the dynamics of the angles $\theta_X$ and $\theta_Y$ inside the well and onto the attractor.

and the function $f_c(\theta_X,\theta_Y)$ models the critical curve.

Let $\phi_l$ and $\phi_r$ denote the maximum angle that the athlete can lean left and right, respectively, and $\phi_f$ and $\phi_b$ denote the maximum angles the athlete can lean forwards and backwards. The actual values of these angles can be found directly from the time series of the three forces $F_X, F_Y$, and $F_Z$, after the conversion into time series of the two angles $\theta_X$ and $\theta_Y$. These are the maximum possible values for which failure does not occur. As shown in Appendix A, the function $f_c(\theta_X,\theta_Y)$ describing the critical curve can be expressed in the form

$$\begin{aligned} f_c(\theta_X,\theta_Y) = &-\phi_l\phi_r\theta_X^2+\phi_l\phi_r(\phi_f+\phi_b)\theta_X-\phi_f\phi_b\theta_Y^2 \\ &+\phi_f\phi_b(\phi_l+\phi_r)\theta_Y+(\phi_b+\phi_f)\theta_X\theta_Y^2 \\ &+(\phi_l+\phi_r)\theta_X^2\theta_Y-(\phi_l+\phi_r)(\phi_b+\phi_f)\theta_X\theta_Y \\ &+I\theta_X^2\theta_Y^2-\phi_f\phi_b\phi_l\phi_r. \end{aligned} \tag{6}$$

If left–right symmetry ($\phi_l=-\phi_r$) is assumed, then Eq. (6) which describes the function $f_c(\theta_X,\theta_Y)$ reduces to

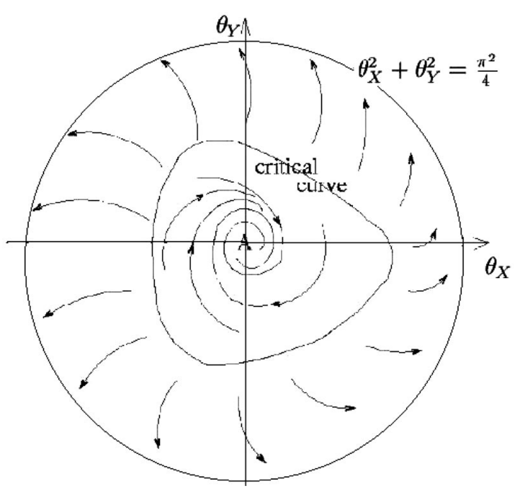


FIG. 5. The critical curve, attracting circle $\theta_X^2+\theta_Y^2=(\pi/2)^2$ and the attracting point $\theta_X=\theta_Y=0$. The figure presents the result of perturbing the center of gravity away from the vertical and watching it spiral onto the attracting fixed point A (corresponding to success), or onto the attracting circle (corresponding to failure).

$$\begin{aligned} f_c(\theta_X,\theta_Y) = &\phi_r^2\theta_X^2-\phi_r^2(\phi_f+\phi_b)\theta_X-\phi_f\phi_b\theta_Y^2 \\ &+(\phi_b+\phi_f)\theta_X\theta_Y^2+I\theta_X^2\theta_Y^2+\phi_f\phi_b\phi_r^2. \end{aligned} \tag{7}$$

The parameter $I$ in Eqs. (6) and (7) governs the curvature of the curve. Numerically it was found that values of $0<I<1$ are a suitable choice for the value of the remaining parameter $I$. With substitution of the above values for the parameters, we obtain the form of the function $f_c(\theta_X,\theta_Y)$ describing the critical curve presented by Eq. (6).

## IV. ANALYSIS

### A. The linear stability of the structures

We investigate here the linear stability of the structures $f_{ax}$, $f_{ay}$, $f_c$, and $f_f$. These structures correspond to the following three fixed points of the system:

(1) $f_{ax}=0$ and $f_{ay}=0$;
(2) $f_c=0$;
(3) $f_f=0$.

In the sections that follow we solve for both the eigenvalues and eigenvectors for the three structures (see also Appendix B).

#### *1. Attracting fixed point $\theta_X=\theta_Y=0$: Case $f_{ax}=f_{ay}=0$*

When $\theta_X=\theta_Y=0$ there is [see Eq. (B1)]

$$\lambda=\phi_f\phi_b\phi_l\phi_r\frac{\pi^2}{8}\{(\alpha+\kappa)\pm\sqrt{(\alpha-\kappa)^2+4\gamma\eta}\}. \tag{8}$$

Thus when $\alpha+\kappa<0$ and $(\alpha-\kappa)^2+4\gamma\eta<0$ we have the required attracting complex fixed point.

Solving the system of Eqs. (B2) and (B3) for the special case of the fixed point $\theta_X=\theta_Y=0$, the eigenvectors can be found to be

$$v_Y=\frac{\kappa-\alpha\pm\sqrt{(\alpha-\kappa)^2+4\gamma\eta}}{2\eta}v_X. \tag{9}$$

#### *2. Repelling critical curve: Case $f_c=0$*

In this case the values of $\theta_X$ and $\theta_Y$ are such that $f_c=0$. There is $\lambda=0$, or [Eq. (B1)]

$$\lambda=-f_f\left\{(\alpha\theta_X+\eta\theta_Y)\frac{\partial f_c}{\partial\theta_X}+(\gamma\theta_X+\kappa\theta_Y)\frac{\partial f_c}{\partial\theta_Y}\right\}, \tag{10}$$

which for a repelling solution requires that, for $\theta_X$ and $\theta_Y$ such that $f_c=0$,

$$(\alpha\theta_X+\eta\theta_Y)\frac{\partial f_c}{\partial\theta_X}+(\gamma\theta_X+\kappa\theta_Y)\frac{\partial f_c}{\partial\theta_Y}<0.$$

From Eqs. (B2) and (B3), the eigenvectors can be found as follows: For $\lambda=0$, there is

$$f_{ax}\cdot f_f\left(\frac{\partial f_c}{\partial\theta_X}v_X+\frac{\partial f_c}{\partial\theta_Y}v_Y\right)=0$$

and

$$f_{ay}\cdot f_f\left(\frac{\partial f_c}{\partial\theta_X}v_X+\frac{\partial f_c}{\partial\theta_Y}v_Y\right)=0,$$

hence for $f_f \neq 0$, $f_{ax} \neq 0$ and $f_{ay} \neq 0$, there is

$$\frac{\partial f_c}{\partial \theta_X} v_X + \frac{\partial f_c}{\partial \theta_Y} v_Y = 0. \tag{11}$$

Special cases:

(a) On the axis $\theta_X = 0$. The eigenvector in this special case is parallel to $\mathbf{v} = \binom{1}{0}$, which is perpendicular to the $\theta_Y$ axis.

(b) On the axis $\theta_Y = 0$. In this special case the eigenvector is parallel to $\mathbf{v} = \binom{0}{1}$, which is perpendicular to the $\theta_X$ axis.

For $\lambda = -f_f\{(\alpha\theta_X + \eta\theta_Y)(\partial f_c/\partial\theta_X) + (\gamma\theta_X + \kappa\theta_Y) \times (\partial f_c/\partial\theta_Y)\}$, there is

$$f_f \frac{\partial f_c}{\partial \theta_Y}\{(\gamma\theta_X + \kappa\theta_Y)v_X - (\alpha\theta_X + \eta\theta_Y)v_Y\} = 0$$

and

$$f_f \frac{\partial f_c}{\partial \theta_X}\{-(\gamma\theta_X + \kappa\theta_Y)v_X + (\alpha\theta_X + \eta\theta_Y)v_Y\} = 0.$$

Hence for $f_f \neq 0$, $\partial f_c/\partial\theta_X \neq 0$, and $\partial f_c/\partial\theta_Y \neq 0$ there is

$$(\gamma\theta_X + \kappa\theta_Y)v_X - (\alpha\theta_X + \eta\theta_Y)v_Y = 0,$$

and thus

$$v_Y = \frac{\gamma\theta_X + \kappa\theta_Y}{\alpha\theta_X + \eta\theta_Y} v_X. \tag{12}$$

Special cases:

(1) On the axis $\theta_X = 0$, there is

(a) point $\theta_Y = \phi_l$,

$$\lambda = -\kappa\phi_l\phi_f\phi_b(\phi_r - \phi_l)\left(\frac{\pi^2}{4} - \phi_l^2\right);$$

(a) point $\theta_Y = \phi_r$,

$$\lambda = -\kappa\phi_r\phi_f\phi_b(\phi_l - \phi_r)\left(\frac{\pi^2}{4} - \phi_r^2\right).$$

For all the above $\theta_X = 0$ solutions it is easy to observe that the strength of the attractor or repeller is governed by $\kappa$, as all the other parameters are fixed.

There is also $v_Y = (\kappa/\eta)v_X$, thus the eigenvector in this special case is parallel to $\mathbf{v} = \binom{1}{\kappa/\eta}$.

(2) On the axis $\theta_Y = 0$, there is

(a) point $\theta_X = \phi_f$

$$\lambda = -\alpha\phi_f\phi_l\phi_r(\phi_b - \phi_f)\left(\frac{\pi^2}{4} - \phi_f^2\right);$$

(a) point $\theta_X = \phi_b$,

$$\lambda = -\alpha\phi_b\phi_l\phi_r(\phi_f - \phi_b)\left(\frac{\pi^2}{4} - \phi_b^2\right).$$

It is easy to observe that, for $\theta_Y = 0$, the strength of the attractor or repeller is governed by $\alpha$.

Also there yields $v_Y = (\gamma/\alpha)v_X$. Therefore the eigenvector in this special case is parallel to $\mathbf{v} = \binom{1}{\gamma/\alpha}$.

### 3. Attracting circle $\theta_X^2 + \theta_Y^2 = \pi^2/4$: Case $f_f = 0$

On the attracting circle $\theta_X^2 + \theta_Y^2 = \pi^2/4$, there is $\lambda = 0$ [Eq. (B1)] or

$$\lambda = 2 f_c\{\alpha\theta_X^2 + \kappa\theta_Y^2 + \theta_X\theta_Y(\eta + \gamma)\}. \tag{13}$$

On the circle $f_f = 0$ there is $f_c > 0$. Thus the circle is attracting only when

$$\alpha\theta_X^2 + \kappa\theta_Y^2 + \theta_X\theta_Y(\eta + \gamma) < 0.$$

Recalling Eqs. (B2) and (B3), the eigenvectors can be found as follows:

For $\lambda = 0$,

$$f_{ax} \cdot f_c\left(\frac{\partial f_f}{\partial \theta_X} v_X + \frac{\partial f_f}{\partial \theta_Y} v_Y\right) = 0,$$

and

$$f_{ay} \cdot f_c\left(\frac{\partial f_f}{\partial \theta_X} v_X + \frac{\partial f_f}{\partial \theta_Y} v_Y\right) = 0.$$

Hence for $f_c \neq 0$, $f_{ax} \neq 0$ and $f_{ay} \neq 0$, there is

$$\theta_X v_X + \theta_Y v_Y = 0. \tag{14}$$

Special cases:

(a) On the axis $\theta_X = 0$.
The eigenvector is parallel to
$$\mathbf{v} = \begin{pmatrix}1\\0\end{pmatrix}.$$

(b) On the axis $\theta_Y = 0$.
The eigenvector is parallel to
$$\mathbf{v} = \begin{pmatrix}0\\1\end{pmatrix}.$$

For $\lambda = f_c\{2\alpha\theta_X^2 + 2\kappa\theta_Y^2 + 2\theta_X\theta_Y(\eta + \gamma)\}$,

$$f_c \frac{\partial f_f}{\partial \theta_Y}((\gamma\theta_X + \kappa\theta_Y)v_X - (\alpha\theta_X + \eta\theta_Y)v_Y) = 0$$

and

$$f_c \frac{\partial f_f}{\partial \theta_X}((\gamma\theta_X + \kappa\theta_Y)v_X - (\alpha\theta_X + \eta\theta_Y)v_Y) = 0.$$

Hence for $f_c \neq 0$, $\partial f_f/\partial\theta_X \neq 0$, and $\partial f_f/\partial\theta_Y \neq 0$, there is

$$(\gamma\theta_X + \kappa\theta_Y)v_X - (\alpha\theta_X + \eta\theta_Y)v_Y = 0,$$

and thus

$$v_Y = \frac{\gamma\theta_X + \kappa\theta_Y}{\alpha\theta_X + \eta\theta_Y} v_X. \tag{15}$$

Special cases:

(a) On the axis $\theta_X = 0$, there are points $\theta_Y = \pm\pi/2$,
$$\lambda = \kappa\frac{\phi_f\phi_b\pi^2}{2}\left\{-\frac{\pi^2}{4} - \phi_l\phi_r + (\phi_l + \phi_r)\left(\pm\frac{\pi}{2}\right)\right\}.$$
As was the case with the $\theta_X = 0$ solution on the critical curve $f_c$, the strength of the attractor or repeller is governed by $\kappa$. Also the eigenvector can be easily proved to be parallel to $\mathbf{v} = \binom{1}{\kappa/\eta}$.

(b) On the axis $\theta_Y=0$, there are points $\theta_X=\pm\pi/2$,

$$\lambda=\alpha\frac{\phi_l\phi_r\pi^2}{2}\left\{-\frac{\pi^2}{4}-\phi_f\phi_b+(\phi_f+\phi_b)\left(\pm\frac{\pi}{2}\right)\right\}.$$

We observe again that, for $\theta_Y=0$, the strength of the attractor or repeller is governed by $\alpha$, as was the case on the critical curve $f_c$. The same way it can be easily seen that the eigenvector in this special case is also parallel to

$$\mathbf{v}=\begin{pmatrix}1\\ \dfrac{\gamma}{\alpha}\end{pmatrix}.$$

### B. A study of the value of parameters $\alpha$, $\eta$, $\gamma$, and $\kappa$

According to the results of the previous sections, for the eigenvalues to be the required ones the following four inequalities should be satisfied, in order of priority [i.e., the attractor at (0,0) is the most important followed by the repelling circle $f_c$, then the attracting circle $f_f$]:

$$\alpha+\kappa<0,\quad (\alpha-\kappa)^2+4\gamma\eta<0, \tag{16}$$

$$(\alpha\theta_X+\eta\theta_Y)\frac{\partial f_c}{\partial\theta_X}+(\gamma\theta_X+\kappa\theta_Y)\frac{\partial f_c}{\partial\theta_Y}<0, \tag{17}$$

$$\alpha\theta_X^2+\kappa\theta_Y^2+\theta_X\theta_Y(\eta+\gamma)<0, \tag{18}$$

where inequality (17) is valid for the points for which $f_c(\theta_X,\theta_Y)=0$ and inequality (18) is valid for the points $f_f(\theta_X,\theta_Y)=0$.

Let us examine the case of $f_c$ at the points where it crosses the axis. There is

(1) for $\theta_X=0$,

$$\theta_Y=\phi_l,\quad \frac{\partial f_c}{\partial\theta_X}=0,\quad \frac{\partial f_c}{\partial\theta_Y}=-\phi_f\phi_b(\phi_l-\phi_r),$$

$$\theta_Y=\phi_r,\quad \frac{\partial f_c}{\partial\theta_X}=0,\quad \frac{\partial f_c}{\partial\theta_Y}=\phi_f\phi_b(\phi_l-\phi_r).$$

So, inequality (17) gives

$$-\kappa\phi_l\phi_f\phi_b(\phi_l-\phi_r)<0,\quad \kappa\phi_r\phi_f\phi_b(\phi_l-\phi_r)<0.$$

(2) For $\theta_Y=0$,

$$\theta_X=\phi_f,\quad \frac{\partial f_c}{\partial\theta_X}=-\phi_l\phi_r(\phi_f-\phi_b),\quad \frac{\partial f_c}{\partial\theta_Y}=0,$$

$$\theta_X=\phi_b,\quad \frac{\partial f_c}{\partial\theta_X}=\phi_l\phi_r(\phi_f-\phi_b),\quad \frac{\partial f_c}{\partial\theta_Y}=0.$$

So inequality (17) gives

$$-\alpha\phi_f\phi_l\phi_r(\phi_f-\phi_b)<0,\quad \alpha\phi_b\phi_l\phi_r(\phi_f-\phi_b)<0.$$

Therefore, as $\phi_f-\phi_b>0$, $\phi_l\phi_f\phi_b>0$, $\phi_r\phi_f\phi_b<0$, $\phi_f\phi_l\phi_r<0$ and $\phi_b\phi_f\phi_r>0$ there is $\alpha<0$ and $\kappa(\phi_l-\phi_r)>0$.

We now examine the case of $f_f$ at the points where it crosses the axis. Let us choose two points on the attracting circle $f_f=0$, namely the points

$$\theta_X=\theta_Y=\pm\sqrt{\frac{\pi^2}{8}}.$$

By substituting these values into the relation (18) we have

$$\alpha+\kappa+\eta+\gamma<0.$$

So the inequalities for the four parameters are

$$\alpha<0, \tag{19}$$

$$\kappa(\phi_r-\phi_l)<0, \tag{20}$$

$$\alpha+\kappa<0, \tag{21}$$

$$(\alpha-\kappa)^2+4\gamma\eta<0\rightarrow\eta\gamma<0, \tag{22}$$

$$\alpha+\kappa+\eta+\gamma<0. \tag{23}$$

## V. APPLICATION OF THE MODEL

From the data of the force platform (after transformation into the angles $\theta_X$ and $\theta_Y$) we have, for the particular athlete (in rads):

$$\phi_f=0.184,$$

$$\phi_b=-0.078,$$

$$\phi_r=0.093,$$

$$\phi_l=-0.117.$$

The angles $\phi_f$, $\phi_b$, $\phi_r$, and $\phi_l$ correspond to the maximum observed angle (in any of the time series for that athlete) that the individual could lean in each direction, respectively, and still correct the perturbation to regain balance. After substitution of the above values, the function $f_c$ which describes the critical curve [Eq. (6)] takes the form

$$\begin{aligned}f_c(\theta_X,\theta_Y)=&0.01088\theta_X^2-0.00115\theta_X+0.01435\theta_Y^2\\&+0.00034\theta_Y+0.10600\theta_X\theta_Y^2-0.2400\theta_X^2\theta_Y\\&+0.00254\theta_X\theta_Y+I\theta_X^2\theta_Y^2-0.00016=0.\end{aligned} \tag{24}$$

Figure 6 shows the above critical curve, together with its idealized, symmetric critical curve (dashed line).

Figure 7 presents a numerically generated example showing the evolution of the following different initial conditions (the angles are expressed in rads):

$$\theta_X(0)=0.07,\quad \theta_Y(0)=0.07,$$

$$\theta_X(0)=-0.05,\quad \theta_Y(0)=-0.05,$$

$$\theta_X(0)=-0.05,\quad \theta_Y(0)=0.05,$$

$$\theta_X(0)=0.07,\quad \theta_Y(0)=-0.07,$$

$$\theta_X(0)=-0.1,\quad \theta_Y(0)=0.1,$$

$$\theta_X(0)=0.1,\quad \theta_Y(0)=0.1,$$

$$\theta_X(0)=0.1,\quad \theta_Y(0)=-0.1,$$

$$\theta_X(0)=-0.1,\quad \theta_Y(0)=-0.1.$$

As can be seen the initial conditions starting inside the critical curve spiral to the attracting fixed point, while those starting outside the critical curve evolve towards the attracting circle.

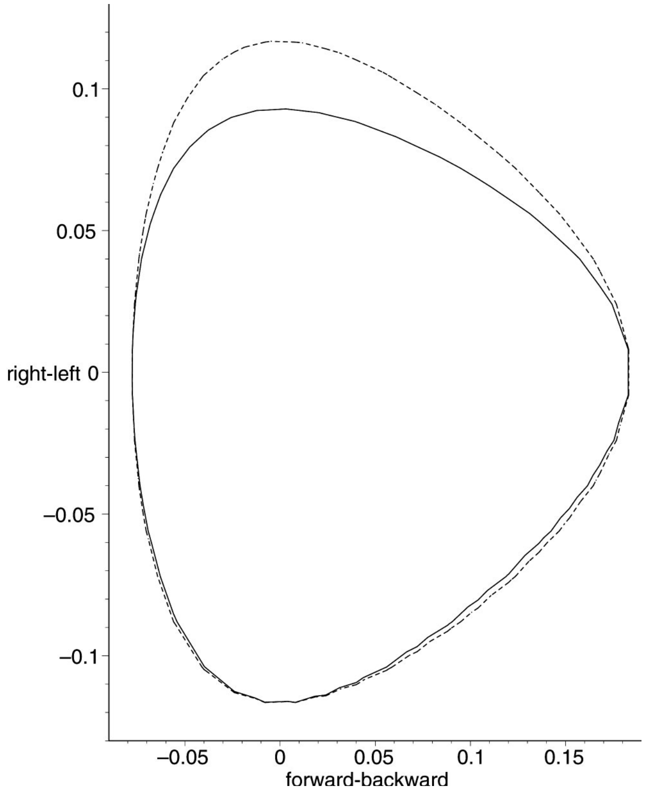


FIG. 6. The critical curve corresponding to Eq. (24) (solid line) and its corresponding idealized symmetric critical curve (dashed line). The horizontal axis represents the angle $\theta_X$, while the vertical axis represents the angle $\theta_Y$; both angles are expressed in rads. For the evaluation of the function the value of the parameter $I$ was chosen to be $I=0.3$.

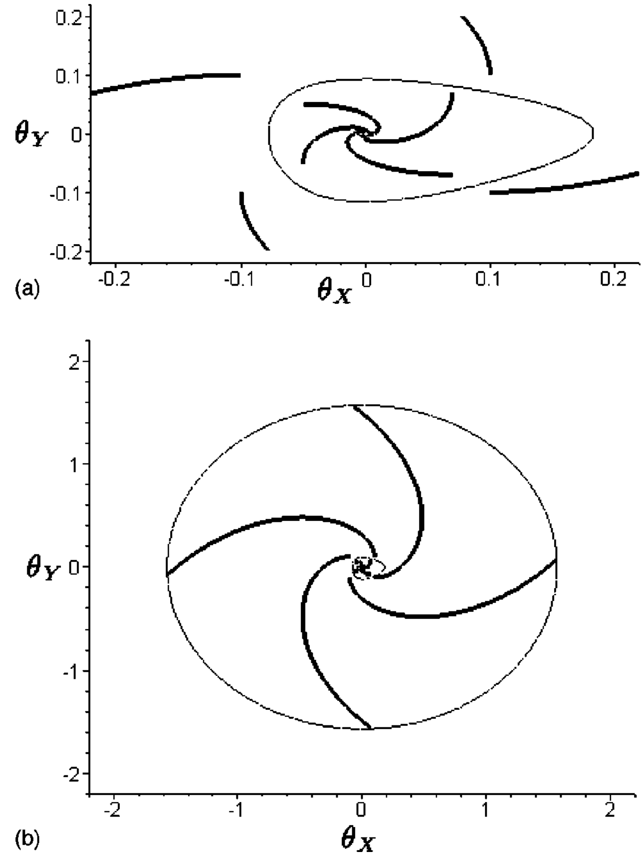


FIG. 7. A numerically generated example showing the evolution of different initial conditions (see text) evolving in the phase space of our model. It is worth noticing that the basin of attraction corresponding to the experimental data (see Fig. 4) is far more irregular and hence the spiral is more complicated than the one shown here; however, it is still a spiral.

## VI. CONCLUSIONS AND PRACTICAL IMPLICATIONS

We present a model of the process by which an athlete, or person in general, regains balance following a perturbation from quiet stance. This model is in the form of a set of coupled vector fields for the angle of the resultant force from the vertical in the mediolateral and anteroposterior directions. We show how two of the main features of the model, the critical curve (i.e., its shape, size, and linear stability) and attracting fixed point (i.e., its linear stability) can be fit to the raw data obtained from the force platform. We also show that the large scale oscillations seen on the time series of the raw data can be due to the center of gravity moving back from the position it was perturbed to, in a spiral-like manner. We simplify the dynamics and do not take into account sway during quiet stance or any of the high frequency oscillations. This enables us to model the underlying motion back onto the attracting fixed point, corresponding to a quiet stance, as that onto a complex sink. The reasons for this simplification are that the amplitudes of motions we consider here are much larger than those considered when analyzing sway during quiet stance.

Organisms attempt to maximize their efficiency in controlling stance. They strive to achieve a control strategy in which minimum energy is expended in the achievement of a stable body configuration (Riccio and Stoffregen[5]). It is common in sport (and also medicine) to periodically test athletes to see whether improvements have occurred resulting from training and to use the results to suggest changes to their existing training methods. Such tests are also commonly used to compare the athletes' performance with accepted standards required for a particular level of performance. With this in mind we make the following four recommendations for how a model such as the one we present here can be used to analyze technique and hence performance (see Stirling and Zakythinaki[35] for more details on this and in particular with regards injury prevention):

(1) Many injuries are caused by nonsymmetric motion resulting from muscle imbalances and differences in the ranges of motion on either side of the body. Such things can easily be observed in our model once the critical curve has been fit (see Fig. 6 for a comparison of a symmetric and a nonsymmetric critical curve). Hence the model can be used to identify and suggest directions for improvement via training.
(2) Improvements in performance will arise if the athlete were able to lean further from the vertical and still be able to correct the perturbation. In our model this would easily be seen as an increase in the size of the basin of attraction and hence the area bound by the critical curve.
(3) Increases in muscular strength resulting from training will lead to the athlete being able to correct larger per-

turbations and do so in less time and with fewer large scale oscillations. In our model this will be seen as an increase in the strength of the attracting fixed point, or in other words a more negative real part of the complex eigenvalues of the attracting fixed point. By tracking changes in the values of the parameters governing this we can track changes in the stability of the athlete.

(4) The methods of analysis and presentation of data used here (i.e., plotting $\theta_x$ against $\theta_y$) can also highlight other phenomena such as the case where an athlete following a perturbation spirals back onto fixed point while favoring one side of the body. This is seen when the center of gravity does not evenly oscillate about the line of symmetry of the body. This can also be used to indicate muscle imbalances and differences in the ranges of motion on either side of the body.

## ACKNOWLEDGMENTS

This work was partially supported by Grants Nos. SB 2000-0075 and SB 2000-0396 from the Secretaría de Estado de Educación y Universidades, Spanish Ministry of Education, Culture and Sports, as well as the Center de Recerca Matemàtica. The authors would like to acknowledge the technical assistance of Ferran Rey Abella of the E.U. Infermeria i Fisioteràpia, F. Blanquerna, Barcelona, regarding the experiment and collection of data.

## APPENDIX A: DERIVATION OF THE FUNCTION $f_c(\theta_X,\theta_Y)$ DESCRIBING THE CRITICAL CURVE

Let us assume that the critical curve is of the general form

$$f_c(\theta_X,\theta_Y)=A\theta_X^2+B\theta_X+C\theta_Y^2+D\theta_Y+G\theta_X\theta_Y^2+H\theta_X^2\theta_Y+I\theta_X^2\theta_Y^2+J\theta_X\theta_Y-E=0.$$

On the curve $f_c(\theta_X,\theta_Y)=0$ there is $\theta_Y=\phi_r,\phi_l$ for $\theta_X=0$ and hence

$$C\phi_l^2+D\phi_l-E=0, \tag{A1}$$

$$C\phi_r^2+D\phi_r-E=0, \tag{A2}$$

while for $\theta_Y=0$ there is $\theta_X=\phi_b,\phi_f$:

$$A\phi_f^2+B\phi_f-E=0, \tag{A3}$$

$$A\phi_b^2+B\phi_b-E=0. \tag{A4}$$

As we are investigating the general condition (i.e., $\phi_r\neq\phi_l$ and $\phi_f\neq\phi_b$) from Eqs. (A1), (A2), (A3), and (A4) we have

$$A=-\frac{E}{\phi_f\phi_b},\quad B=E\frac{\phi_f+\phi_b}{\phi_f\phi_b},$$

$$C=-\frac{E}{\phi_l\phi_r},\quad D=E\frac{(\phi_l+\phi_r)}{\phi_l\phi_r}. \tag{A5}$$

For the curve to be perpendicular to the axes when it crosses them, there should be

$$\frac{\partial\theta_Y}{\partial\theta_X}=0,\quad \text{for}\quad \theta_X=0\quad\text{and}\quad \theta_Y=\phi_l,\phi_r, \tag{A6}$$

$$\frac{\partial\theta_X}{\partial\theta_Y}=0,\quad \text{for}\quad \theta_Y=0\quad\text{and}\quad \theta_X=\phi_b,\phi_f. \tag{A7}$$

Let $E=\phi_l\phi_r\phi_f\phi_b$. The system of Eqs. (A5), (A6), and (A7) gives for the parameters of the curve the solutions:

$$A=-\phi_l\phi_r,\qquad B=\phi_l\phi_r(\phi_f+\phi_b),$$

$$C=-\phi_f\phi_b,\qquad D=\phi_f\phi_b(\phi_l+\phi_r),$$

$$G=\phi_b+\phi_f,\qquad H=\phi_l+\phi_r,$$

$$J=-(\phi_l+\phi_r)(\phi_b+\phi_f),\quad E=\phi_l\phi_r\phi_f\phi_b.$$

It is worth noticing that if we recall that

(a) the values of $\phi_l,\phi_b$ are less than zero while the values of $\phi_r,\phi_f$ are greater than zero;
(b) according to the model there is $\phi_b+\phi_f>0$;
(c) $\phi_l$ is approximately equal to $-\phi_r$,

then we have

$$A>0,\quad B<0,$$

$$C>0,\quad D\approx 0,$$

$$G>0,\quad H\approx 0,$$

$$J\approx 0,\quad E>0.$$

## APPENDIX B: DERIVATIVES, EIGENVALUES, AND EIGENVECTORS

Below we give an analytical expression for the calculation of the eigenvalues λ, the corresponding eigenvectors

$$\mathbf{v}=\begin{pmatrix} v_X \\ v_Y \end{pmatrix},$$

as well as the derivatives

$$\frac{\partial\dot\theta_X}{\partial\theta_X},\quad \frac{\partial\dot\theta_X}{\partial\theta_Y},\quad \frac{\partial\dot\theta_Y}{\partial\theta_X},\quad \frac{\partial\dot\theta_Y}{\partial\theta_Y},$$

and the derivatives

$$\frac{\partial f_c}{\partial\theta_X}\quad\text{and}\quad\frac{\partial f_c}{\partial\theta_Y}.$$

The Jacobian matrix is

$$J=\begin{pmatrix} \dfrac{\partial\dot\theta_X}{\partial\theta_X} & \dfrac{\partial\dot\theta_X}{\partial\theta_Y} \\[2ex] \dfrac{\partial\dot\theta_Y}{\partial\theta_X} & \dfrac{\partial\dot\theta_Y}{\partial\theta_Y} \end{pmatrix}$$

and we have

$$\lambda=\frac{\dfrac{\partial\dot\theta_X}{\partial\theta_X}+\dfrac{\partial\dot\theta_Y}{\partial\theta_Y}\pm\sqrt{\left(\dfrac{\partial\dot\theta_X}{\partial\theta_X}-\dfrac{\partial\dot\theta_Y}{\partial\theta_Y}\right)^2+4\dfrac{\partial\dot\theta_X}{\partial\theta_Y}\dfrac{\partial\dot\theta_Y}{\partial\theta_X}}}{2}, \tag{B1}$$

$$\left(\frac{\partial \dot{\theta}_X}{\partial \theta_X} - \lambda\right) v_X + \frac{\partial \dot{\theta}_X}{\partial \theta_Y} v_Y = 0, \tag{B2}$$

and

$$\frac{\partial \dot{\theta}_Y}{\partial \theta_X} v_X + \left(\frac{\partial \dot{\theta}_Y}{\partial \theta_Y} - \lambda\right) v_Y = 0. \tag{B3}$$

The derivatives can be written in the following form:

$$\frac{\partial \dot{\theta}_X}{\partial \theta_X} = f_c . f_f \frac{\partial f_{ax}}{\partial \theta_X} + f_{ax} . f_c \frac{\partial f_f}{\partial \theta_X} + f_{ax} . f_f \frac{\partial f_c}{\partial \theta_X},$$

$$\frac{\partial \dot{\theta}_X}{\partial \theta_Y} = f_c . f_f \frac{\partial f_{ax}}{\partial \theta_Y} + f_{ax} . f_c \frac{\partial f_f}{\partial \theta_Y} + f_{ax} . f_f \frac{\partial f_c}{\partial \theta_Y},$$

$$\frac{\partial \dot{\theta}_Y}{\partial \theta_X} = f_c . f_f \frac{\partial f_{ay}}{\partial \theta_X} + f_{ay} . f_c \frac{\partial f_f}{\partial \theta_X} + f_{ay} . f_f \frac{\partial f_c}{\partial \theta_X},$$

$$\frac{\partial \dot{\theta}_Y}{\partial \theta_Y} = f_c . f_f \frac{\partial f_{ay}}{\partial \theta_Y} + f_{ay} . f_c \frac{\partial f_f}{\partial \theta_Y} + f_{ay} . f_f \frac{\partial f_c}{\partial \theta_Y},$$

where

$$\frac{\partial f_{ax}}{\partial \theta_X} = -\alpha, \quad \frac{\partial f_{ax}}{\partial \theta_Y} = -\eta,$$

$$\frac{\partial f_{ay}}{\partial \theta_X} = -\gamma, \quad \frac{\partial f_{ay}}{\partial \theta_Y} = -\kappa,$$

$$\begin{aligned}\frac{\partial f_c}{\partial \theta_X} = & -2\phi_l\phi_r\theta_X + \phi_l\phi_r(\phi_f + \phi_b) + (\phi_b + \phi_f)\theta_Y^2 \\ & + 2(\phi_l + \phi_r)\theta_X\theta_Y - (\phi_l + \phi_r)(\phi_b + \phi_f)\theta_Y \\ & + 2I\theta_X\theta_Y^2,\end{aligned}$$

and

$$\begin{aligned}\frac{\partial f_c}{\partial \theta_Y} = & -2\phi_f\phi_b\theta_Y + \phi_f\phi_b(\phi_l + \phi_r) + 2(\phi_b + \phi_f)\theta_X\theta_Y \\ & + (\phi_l + \phi_r)\theta_X^2 - (\phi_l + \phi_r)(\phi_b + \phi_f)\theta_X + 2I\theta_X^2\theta_Y,\end{aligned}$$

$$\frac{\partial f_f}{\partial \theta_X} = -2\theta_X,$$

$$\frac{\partial f_f}{\partial \theta_Y} = -2\theta_Y.$$


[1] H. Kantz and T. Schreiber, *Nonlinear Time Series Analysis* (Cambridge University Press, Cambridge 1997).
[2] J. Guckenheimer and P. Holmes, *Nonlinear Oscillations, Dynamical Systems, and Bifurcations of Vector Fields* (Springer-Verlag, New York, 1983).
[3] L. Marin, B. G. Bardy, and R. J. Bootsma, ''Level of gymnastic skill as an intrinsic constraint on postural coordination,'' J. Sports Sci. **17**, 615–626 (1999).
[4] N. Vuillerme, F. Danion, L. Marin, A. Boyadjian, J. M. Prieur, I. Weise, and V. Nougier, ''The effect of expertise in gymnastics on postural control,'' Neurosci. Lett. **303**, 83–86 (2001).
[5] G. E. Riccio and T. A. Stoffregen, ''Affordances as constraints on the control of stance,'' Human Movement Sci. **7**, 265–300 (1988).
[6] J. Mester, ''Movement control and balance in earthbound movements,'' in *Biomechanics and Biology of Movement* (Human Kinetics, Champaign, IL, 2000).
[7] C. C. Chow and J. J. Collins, ''Pinned polymer model of posture control,'' Phys. Rev. E **52**, 907–912 (1995).
[8] C. C. Chow, M. Lauk, and J. J. Collins, ''The dynamics of quasistatic postural control,'' Human Movement Sci. **18**, 725–740 (1999).
[9] J. J. Collins and C. J. De Luca, ''Open-loop and closed-loop control of posture: A random walk analysis of center of pressure,'' Exp. Brain Res. **95**, 308–318 (1993).
[10] J. J. Collins and C. J. De Luca, ''Random walking while quiet standing,'' Phys. Rev. Lett. **73**, 764–767 (1994).
[11] J. J. Collins and C. J. De Luca, ''The effects of visual input on open-loop and closed-loop postural control mechanisms,'' Exp. Brain Res. **103**, 151–163 (1995).
[12] J. J. Collins and C. J. De Luca, ''Upright, correlated random walk: A statistical-biomechanics approach to the human postural control system,'' Chaos **5**, 57–63 (1995).
[13] T. D. Frank, A. Daffertshofer, and P. J. Beek, ''Multivariate Ornstein–Uhlenbeck processes with mean-field dependent coefficients: Application to postural sway,'' Phys. Rev. E **63**, 011905 (2001).
[14] M. Lauk, C. C. Chow, A. E. Pavlik, and J. J. Collins, ''Human balance out of equilibrium: Nonequilibrium statistical mechanics of posture control,'' Phys. Rev. Lett. **80**, 413–416 (1998).
[15] A. Priplata, J. Niemi, M. Salen, J. Harry, L. A. Lipsitz, and J. J. Collins, ''Noise-enhanced human balance control,'' Phys. Rev. Lett. **89**, 238101 (2002).
[16] M. A. Riley, S. Wong, S. Mitra, and M. T. Turvey, ''Common effects of touch and vision on postural parameters,'' Exp. Brain Res. **117**, 165–170 (1997).
[17] R. Balasubramaniam and A. M. Wing, ''The dynamics of standing balance,'' Trends Cogn. Sci. **6**, 531–536 (2002).
[18] O. Oullier, B. G. Bardy, T. A. Stoffregen, and R. J. Bootsma, ''Postural coordination in looking and tracking tasks,'' Human Movement Sci. **21**, 147–167 (2002).
[19] S. Yoneda and K. Tokumasu, ''Frequency analysis of body sway in the upright posture: Statistical study in cases of peripheral vestibular disease,'' Acta Otolaryngol. Suppl. (Stockh) **102**, 87–92 (1986).
[20] D. A. Winter, F. Prince, J. S. Frank, C. Powell, and K. F. Zabjek, ''Unified theory regarding A/P and M/L balance in quiet stance,'' J. Neurosci. **75**, 2334–2343 (1996).
[21] R. Balasubramaniam, M. A. Riley, and M. T. Turvey, ''Specificity of postural sway to the demands of a precision task,'' Gait Posture **11**, 12–24 (2000).
[22] L. M. Nashner, ''Adapting reflexes controlling the human posture,'' Exp. Brain Res. **26**, 59–72 (1976).
[23] L. M. Nashner and G. McCollum, ''The organization of postural movements: A formal basis and experimental synthesis,'' Behav. Brain Sci. **26**, 135–172 (1985).
[24] F. B. Horak and L. M. Nashner, ''Central programming of postural movements: Adaptation to altered support-surface configurations,'' J. Neurophysiol. **55**, 1369–1381 (1986).
[25] G. McCollum and T. K. Leen, ''Form and exploration of mechanical stability limits in erect stance,'' J. Motor Behav. **21**, 225–244 (1989).
[26] B. G. Bardy, L. Marin, T. A. Stoffregen, and R. J. Bootsma, ''Postural coordination modes considered as emergent phenomena,'' J. Exp. Psychol. Hum. Percept. Perform. **25**, 1284–1301 (1999).
[27] B. G. Bardy, O. Oullier, R. J. Bootsma, and T. A. Stoffregen, ''Dynamics of human postural transitions,'' J. Exp. Psychol. Hum. Percept. Perform. **28**, 499–514 (2002).
[28] H. Lekhel, A. R. Marchand, C. Assaiante, J. Cremieux, and B. Amblard, ''Cross-correlation analysis of the lateral hip strategy in umperturbed stance,'' NeuroReport **10**, 1293–1296 (1994).
[29] J. Massion, *Cerveau et Motricité* (Presses Universitaires de France, Paris, 1997).
[30] S. Bouisset, ''Relations entre le support postural et le mouvement intentionnel: Approche biomécanique,'' Arch. Int. Physiol., Biochim. Biophys. **99**, A77–A92 (1991).
[31] K. M. Newell, ''Constraints on the development of coordination,'' in *Motor Development in Children: Aspects of Coordination and Control*, edited by M. G. Wade and H. T. A. Whiting (Martinus Nijhoff, Boston, 1986), pp. 341–360.
[32] J. A. S. Kelso, *Dynamic Patterns: The Self-Organization of Brain and Behavior (Complex Adaptive Systems)* (MIT Press, Cambridge, 1995).

[33] N. A. Bernstein, *The Coordination and Regulation of Movement* (Pergamon, New York, 1967).
[34] K. J. Sims and S. G. Brauer, ''A rapid upward step challenges mediolateral postural stability,'' Gait Posture **12**, 217–224 (2000).
[35] J. R. Stirling and M. S. Zakynthinaki, ''A model of stability and balance,'' *Lecture Notes of ICB Seminars*, 2003 (to be published).
[36] T. A Stoffregen, R. J. Pagulayan, B. G. Bardy, and L. J. Hettinger, ''Modulating postural control to facilitate visual performance,'' Human Movement Sci. **19**, 203–220 (2000).
[37] M. S. Zakynthinaki, adaptation of V. Ng-Thow-Hing and P. Faloutsos, ''Dynamic Animation and Control Environment (Dance),'' version 1.0, University of Toronto, 2000, UPC (2002).